Director Fields on Manifolds, a Diffuse Domain Approach

March 31, 2015

Abstract

1 Introduction

2 Director Field

Throughout this paper we consider a director field to be a smooth(beside isolated points) vectorfield $\mathbf{p}$ with unit length on a singely connected subset of $\mathcal{R}^3$. For the special case of surfaces S we also require $\mathbf{p} \in TS$ or $\mathbf{p} \cdot \mathbf{n} = 0$($\mathbf{n}$ surface normal).

The established modelling of director field dynamics $\mathbf{p}(\mathbf{x}, t)$ bases on definition of a free energy(E)/energy density(e) with dynamics driven by a gradient flow $\frac{\partial \mathbf{p}}{\partial t} = -\frac{\delta e}{\delta \mathbf{p}}$.

A well known defintion of such a energy is the elastic Frank Oseen energy(cite 3), penalizing three basic deformations(splay, twist and bend) in the director

$$E = \int_\Omega \underbrace{\frac{K_1}{2}(\nabla \cdot \mathbf{p})^2}_{\text{splay}} + \underbrace{\frac{K_2}{2}(\mathbf{p} \cdot [\nabla \times \mathbf{p}])^2}_{\text{twist}} + \underbrace{\frac{K_3}{2}\|\mathbf{p} \times [\nabla \times \mathbf{p}]\|^2}_{\text{bend}} \, \mathbf{d}\Omega$$

Applying the widely used One Constant Approximation(cite 3) $K_1 = K_2 = K_3 = K_o$ and incorporating $\|\mathbf{p}\| = 1$ allows us to simplify this energy functional to

$$E = \int_\Omega \frac{K_0}{2}\|\nabla \mathbf{p}\|_F^2 \, \mathbf{d}\Omega \tag{1}$$

$$\|\nabla \mathbf{p}\|_F^2 = \sum_{ij} (\nabla_i \mathbf{p}_j)^2 \tag{2}$$

For time beeing we consider only passive dynamics(without external forces, continously driving the system) relaxating from an intial state to the equilibrium. Please note that in this type of dynamics the resting points/equilibrium

manifold of the system are also defined by a solution of a constraint minimization problem

$$\begin{aligned} &\text{find } \mathbf{p} \quad \text{such that :} && (3)\\ &\qquad \min E(\mathbf{p}) \ \text{ and} && (4)\\ &\qquad \|\mathbf{p}\| = 1 && (5)\\ &\qquad \text{furthermore for surface } \mathbf{p}\cdot\mathbf{n} = 0 && (6) \end{aligned}$$

The solution to (3) is smooth beside a zero-meassured set of isolated points[1] called defects $\{\tilde{\mathbf{x}}_i\}_i$. At this points at least one of the state constraints on $\mathbf{p}$ is void. The amount of defects dictated by choosen boundary conditions and topological properties of the domain/surface. Further this defects can be endowed with a characteristic number, called Index $\mathbf{Ind}(\tilde{\mathbf{x}})$ (cite). For director fields exists three basic types called vortex, source/sink and saddle. In special case of closed surfaces Poincare Hopf theorem(cite) states that any director field must satisfy $\sum_i \mathbf{Ind}(\tilde{\mathbf{x}}_i) = \mathrm{E}(S)$, where $\mathrm{E}(S)$ is the Euler characteristic of the surface(an overview of Euler characteristics see appendix).

Figure 1: types of defects: vortex, source/sink and saddle point

3 Diffuse Domain Modelling

What is Diffuse Domain: The proposed approach bases on the diffuse interface approach for domain description. Central idea in our approach is to embed the relevant domain Ω in a favorable shaped domain $\tilde{\Omega}$ and to approximate the boundary between Ω and $\tilde{\Omega}\setminus\Omega$ by a diffuse interface. Using a suitable smooth phase field function we can asymptotically express the charcteristic function χ_Ω by

$$\begin{aligned} \phi(\mathbf{x}) &= \frac{1}{2}\left(\tanh\left(\frac{d(\mathbf{x},\Omega)}{2\epsilon_\phi}\right)\right)\\ \chi_\Omega(\mathbf{x}) &= \lim_{\epsilon_\phi\to 0}\phi(\mathbf{x}) \end{aligned}$$

Motivation: Main advantage of this kind of numerical approach is that surfaces can be defined easyly(by a suitable distance field) and we do not have to discriminate between surface or domain. This comes in handy for surface/-domain evolutions involving strong deformations or topological changes.

Modell Equations Beside this implicite treatment of the domain we follow the explicit domain approach and enforce the constraints on $\mathbf{p}$ by using penality terms. Namely we add following terms to the energy functional

$$\begin{aligned} &\phi\frac{K_n}{4}\left(\|\mathbf{p}\|^2-1\right)^2\\ &\qquad \phi\frac{K_t}{2}\|\mathbf{p}\cdot\mathbf{n}\|^2 \ , \ \mathbf{n} = \frac{\nabla\phi}{|\nabla\phi|} \end{aligned}$$

Both penality Terms have been restricted to the relevant domain, which allows us to negelect $\mathbf{p} = 0 \ \forall \mathbf{x} \notin \Omega$ and prescribe homogeneous Neumann boundary conditions on the containing domain $\Omega \subset \tilde{\Omega}$ ($\tilde{\Omega}$ ussually a box shaped domain).

$$E = \int_{\Omega} \phi \frac{K_0}{2} \|\nabla \mathbf{p}\|_F^2 + \phi \frac{K_n}{4} \left(\|\mathbf{p}\|^2 - 1 \right)^2 + \phi \frac{K_t}{2} \|\mathbf{p} \cdot \mathbf{n}\|^2 \, \mathbf{d}\Omega \tag{7}$$

With this extended free energy functional the evolution equations reads as

$$\tilde{\phi} \frac{\partial \mathbf{p}}{\partial t} - \tilde{\phi} K_o \triangle \mathbf{p} \tag{8}$$

$$+\phi K_t \left(\frac{\nabla \phi}{|\nabla \phi|} \otimes \frac{\nabla \phi}{|\nabla \phi|}^T \right) \cdot \mathbf{p} + \phi K_n \left(\|\mathbf{p}\|^2 - 1 \right) \mathbf{p} = \quad 0 \quad \tilde{\Omega} \tag{9}$$

$$\frac{\partial \mathbf{p}}{\partial \mathbf{n}} = \quad 0 \quad \tilde{\Gamma} \tag{10}$$

For numerical solution procedures the phase has been regularized for time derivative and laplace term ($\tilde{\phi} = \max(\phi, 10e-4)$) and a linearization of $\left(\|\mathbf{p}\|^2 - 1 \right) \mathbf{p}$ has been applied, for details see Appendix.

Demarcated numerical approximations between explicit domain and spherical harmonics modelling(detailes descripiton of these methods see appendix A).

- spherical harmonics: $\mathbf{p} \in TS$, so single penality term for $\|\mathbf{p}\| = 1$
- explicit domain: $\mathbf{p} \in \mathcal{R}^3$, penality terms for $\|\mathbf{p}\| = 1$ and tangential direction $\mathbf{p} \cdot \mathbf{n} = 0$
- diffuse domain: dynamics as in explicit domain(two penality terms) but domain is asymptotically described by phasefield

To solve the approaches of explicit and diffuse domain we use finite Elements on hierarchic adaptive meshes provided by `AMDiS` .

4 Modell Validation - Minimal Energy Configurations on Unit Sphere

We compare the modell with analytical known directorfield with minimal defect configuration of source sink type on the unit sphere. For the unit sphere a energy minimal director field satisfying (3) with source/sink defect configuration(along z axis) can be described by

$$\mathbf{p}(\mathbf{x}) \quad = \frac{1}{\sqrt{1-\mathbf{x}_3^2}} \begin{bmatrix} \mathbf{x}_1 \mathbf{x}_3 \\ \mathbf{x}_2 \mathbf{x}_3 \\ \mathbf{x}_3^2 - 1 \end{bmatrix}$$

To investigate convergence of out modell torwards this state we consider two asymptotics. First asymptotic we let $\epsilon_\phi \to 0$ to approach the explicit surface/sharp interface limit and second we ramp up $K_t = K_n$ to approach the

constraints $\|\mathbf{p}\| = 1$ and $\mathbf{p} \cdot \mathbf{n} = 0$. Throughout the calculations we keep a fixed $K_o = 1$
We perform several simulations starting at noise director field until engery relaxes. From this simulations we select the minimal energy director field configurations exhibiting the source/sink defect configuration. Due to the rotational invariance of the analytical configurations we rotate the evaluated configuration to match the defect axis(source-sink) with z-Axis and compute the L^2 difference between analytical and evaluated configuration.

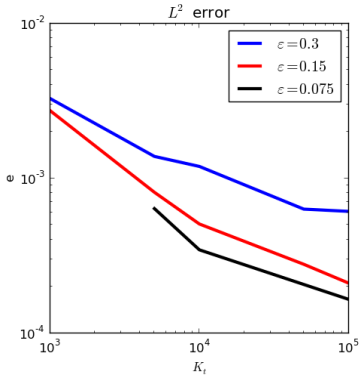

Figure 2: L^2 error vs $K_t = K_n \to \infty$ and $\epsilon_\phi \to 0$

5 Modell Validation - Defect Trajectories on Unit Sphere

As second approach to validate our modell we compare defect trajectories on the unit sphere. By choosing a suitable initial value we define a predictable/well defined final equilibrium state. For comparision we use two established numerical schemes, namely the epxlicit domain formulation and the formulation in spherical harmonics.
As initial Value we define a non minimum energy director field with four defects summing up to the correct topological charge of 2. Namely two sinks(each +1), one source +1 and a saddle point −1 arranged on the great circle of the xy plane. To prescribe the final state we position the saddle point a bit closer($\tilde{\lambda}$) to one sink.
This initial value is obtained by evaluating a preliminary director field $\mathbf{e}$ which is projected into tangential space and normalized afterwards.

$$\begin{array}{rcl} |x_2| \geq \cos\frac{\pi}{4} & : & \mathbf{e} = [-x_1, 0, -x_3]^T \\ x_1 \geq \cos\frac{\pi}{4} & : & \mathbf{e} = [0, x_2, x_3]^T \\ x_1 \leq -\cos\frac{\pi}{4} & : & \mathbf{e} = \left[0, \sin\left(\pi\left(x_2 - \tilde{\lambda}\right)\right), -\sin\left(\pi x_3\right)\right]^T \\ \text{otherwise} & : & \mathbf{e} = \left[|x_2/\cos\frac{\pi}{4}| - 1, x_2/\cos\frac{\pi}{4}, 0\right]^T \end{array}$$

This initial configuration will converge to a minimum energy configuration consiting of a source and sink configuration(still located in XY plane). In the

transient saddle point and the closer sink will annihilate each other.

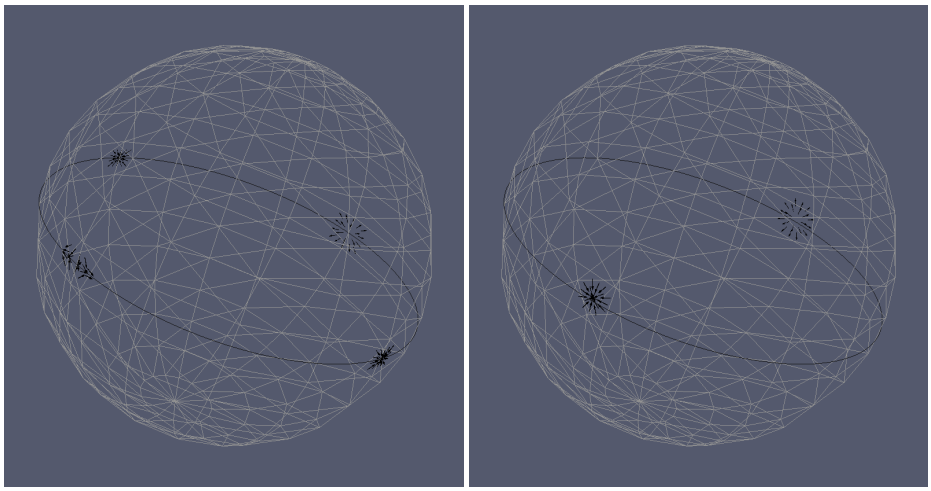

Figure 3: intial and final defects on sphere

In the modell we use penality coefficients as $K_o = 1$ and $K_t = K_n = 1000$, and for the initial value $\tilde{\lambda} = 0.01$
To compare the results of the three modells we plot the trajectories of the four defects in the XY plane via the azimuthal angle φ_i over time

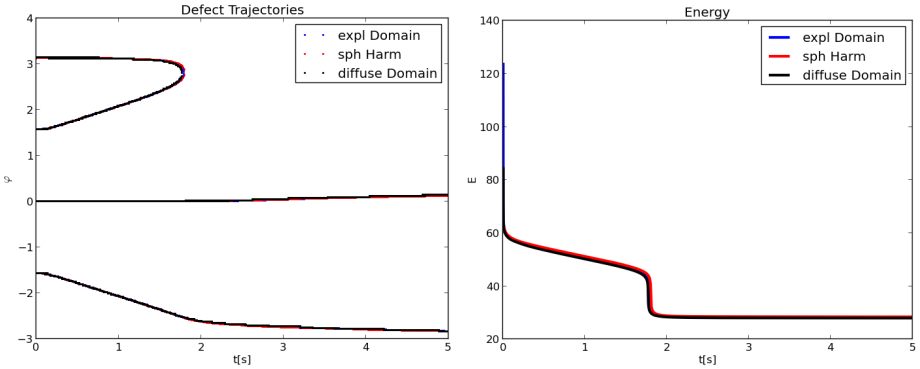

Figure 4: Defect Trajectories in XYplane, Energies

- dynamics of defects match: critical event of annihilation of saddle and source defect is reproduced, final configurations match
- energy transients match

6 Application

6.1 Interplay Curvature and Defect Type on bounded Manifold

quantitative interaction between curvature and defect position To get a quantitative description of the interaction of curvature an defects described in [1] we perform several simulations for a single defect on a bounded plane with a single gaussian bump. The Defect is prescribed by the boundary conditions.

Before starting this ivestigaten we point out that the interaction of defect and curvature dependes on the type of the defect(see fig 5,6). Here we have positioned a gaussian bump at several positions of the plane for a single vertex and a saddle defect. While the vertex defect is attracted to domains with positive Gaussian curvature(and strictly avoids domains with negative curvature) the saddle defect acts contrary.

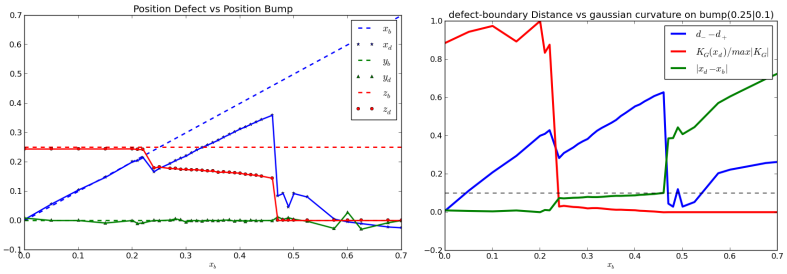

Figure 5: Vortex Defect: Defect Position and Curvature

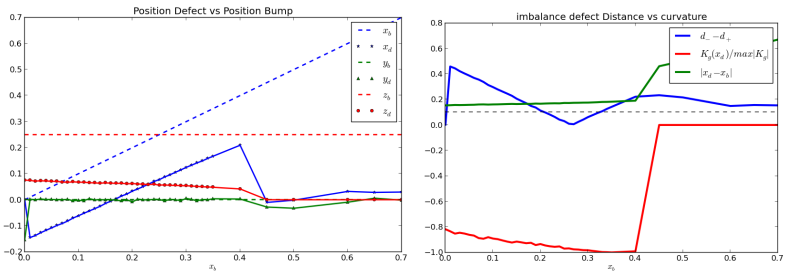

Figure 6: Saddle Defect: Defect Position and Curvature

orientation fields vs flow fields on surfaces compare to results of [2] [3]

6.2 Surface Evolution and Defect Position

Sphere to Ellipsoid and Defect Repositioning

coupling Cahn Hilliard and Orientation Fields

A Orientation Fields on Unit Sphere by Spherical Harmonics and Explicit Domain Modelling

B Linearization of Diffuse Domain Evolution Equations

$$\begin{aligned} & \left(\|\mathbf{p}\|^2 - 1\right)\mathbf{p}_i \\ \approx\ & \|\tilde{\mathbf{p}}\|^2\tilde{\mathbf{p}}_i - \tilde{\mathbf{p}}_i + \left[\nabla\left(\|\tilde{\mathbf{p}}\|^2\tilde{\mathbf{p}}_i - \tilde{\mathbf{p}}_i\right)\right](\mathbf{p}_i - \tilde{\mathbf{p}}_i) \\ =\ & \sum_j \left[\tilde{\mathbf{p}}_j^2\mathbf{p}_i + 2\tilde{\mathbf{p}}_j\tilde{\mathbf{p}}_i\mathbf{p}_j\right] - \mathbf{p}_i - \sum_j \left[2\tilde{\mathbf{p}}_i\tilde{\mathbf{p}}_j^2\right] \end{aligned}$$

C Euler Characteristics for Surfaces

Table 1: topological charge for several surfaces

References

[1] Mark J. Bowick and Luca Giomi. Two-dimensional matter: order, curvature and defects. *Advances in Physics*, 58(5):449–563, 2009.

[2] Axel Voigt Sebastian Reuther. The interplay of curvature and vortices in flow on curved surfaces. 2014.

[3] Ari M. Turner, Vincenzo Vitelli, and David R. Nelson. Vortices on curved surfaces. *Rev. Mod. Phys.*, 82:1301–1348, Apr 2010.